

# Solution structure, dynamics, and hydrodynamics of the cross-reactive birch pollen allergen Bet v 4 reveal a monomeric calmodulin-like 2 EF-hand assembly

Philipp Neudecker, Jörg Nerkamp, Anke Eisenmann, Thomas Lauber, Katrin Lehmann, Kristian Schweimer, Stephan Schwarzinger and Paul Rösch  
Lehrstuhl für Struktur und Chemie der Biopolymere, Universität Bayreuth, Bayreuth, Germany  
Phone: +49-921-553869; Fax: +49-921-553544; E-mail: philipp.neudecker@uni-bayreuth.de

Due to the high IgE cross-reactivity among the polcalcin family of pollen allergens, which share more than 70 % sequence identity, many patients are polysensitized to various plant pollens. To provide a basis for examining the cross-reactivity on a structural level, we determined the high-resolution three-dimensional structure of the  $\text{Ca}^{2+}$ -bound 9.4 kDa birch pollen allergen Bet v 4 in solution by heteronuclear multidimensional NMR spectroscopy. An antiparallel  $\beta$ -sheet formed by a short  $\beta$ -strand each pairs the 2 EF-hands with 2  $\alpha$ -helices enclosing a  $\text{Ca}^{2+}$  binding loop each. The interhelical angles closely resemble  $\text{Ca}^{2+}$ -bound calmodulin. A coordination of each of the 2  $\text{Ca}^{2+}$  ions by 7 O atoms at the vertices of a pentagonal bipyramid as in calmodulin is consistent with the experimental data, a water molecule H-bonded to a slowly exchanging serine OH group contributes the remaining coordination site. The linker between the EF-hands and the COOH-terminal  $\alpha$ -helix show increased flexibility in NMR relaxation experiments. Unlike Phl p 7 from timothy grass, which was recently shown to adopt a domain-swapped dimeric structure in crystalline form, the rotational diffusion correlation times from NMR relaxation and the hydrodynamic radii from NMR translational diffusion and analytical ultracentrifugation indicate that both apo and holo Bet v 4 are predominantly monomeric in solution near pH 6 up to millimolar concentrations, with dimer fractions of 10 to 15 % as determined by mass spectroscopy and analytical ultracentrifugation, raising the question of the physiological and immunological significance of the dimeric form of these polcalcins, whose physiological function is still unknown. The close structural homology to calmodulin suggests a regulatory rather than a  $\text{Ca}^{2+}$ -buffering function for Bet v 4. The reduced helicity and chemical shift dispersion of the CD and NMR spectra of Bet v 4 in the absence of  $\text{Ca}^{2+}$ , respectively, indicate a reversible structural transition explaining the reduced IgE binding capacity of apo Bet v 4. The hypothesis that the  $\text{Ca}^{2+}$  binding sites constitute IgE epitopes would not only provide a straightforward explanation for the IgE cross-reactivity and the ability to crosslink 2 IgE molecules by the 2  $\text{Ca}^{2+}$  binding sites, but also suggests that canonical monomers and domain-swapped dimers may be of similar allergenicity.

## Introduction

Birch pollinosis is one of the prevailing allergic diseases in Northern and Central Europe and Northern America, causing clinical syndromes like hay fever, asthma, and dermatitis. The 17.4 kDa major birch pollen allergen Bet v 1 is responsible for IgE antibody binding in more than 95 % of birch pollinotics, but approximately 10 to 20 % of the patients also show IgE reactivity to the 9.4 kDa minor birch pollen allergen Bet v 4<sup>1,2</sup>. Bet v 4 belongs to the polcalcin family of small acidic intracellular two EF-hand  $\text{Ca}^{2+}$  binding pollen allergens and most Bet v 4 specific IgE antibodies cross-react with other polcalcins like Aln g 4 from alder, Ole e 3 from olive, Syr v 3 from lilac, Bra n 1 and Bra n 2 from rapeseed, Bra r 1 and Bra r 2 from turnip rape, Phl p 7 from timothy grass, and Cyn d 7 from bermuda grass (Fig. 1). The physiological function of these allergens is still unknown, although a role in the regulation of pollen tube growth, which involves a tip-focused  $\text{Ca}^{2+}$  gradient, has been proposed. Recently, the three-dimensional structure of holo Phl p 7 was determined by X-ray crystallography<sup>3</sup> and surprisingly revealed a domain-swapped dimeric quaternary structure instead of the canonical intramolecular EF-hand pairing observed in EF-hand proteins like parvalbumin, calmodulin, troponin C, and calbindin  $\text{D}_{9k}$ .

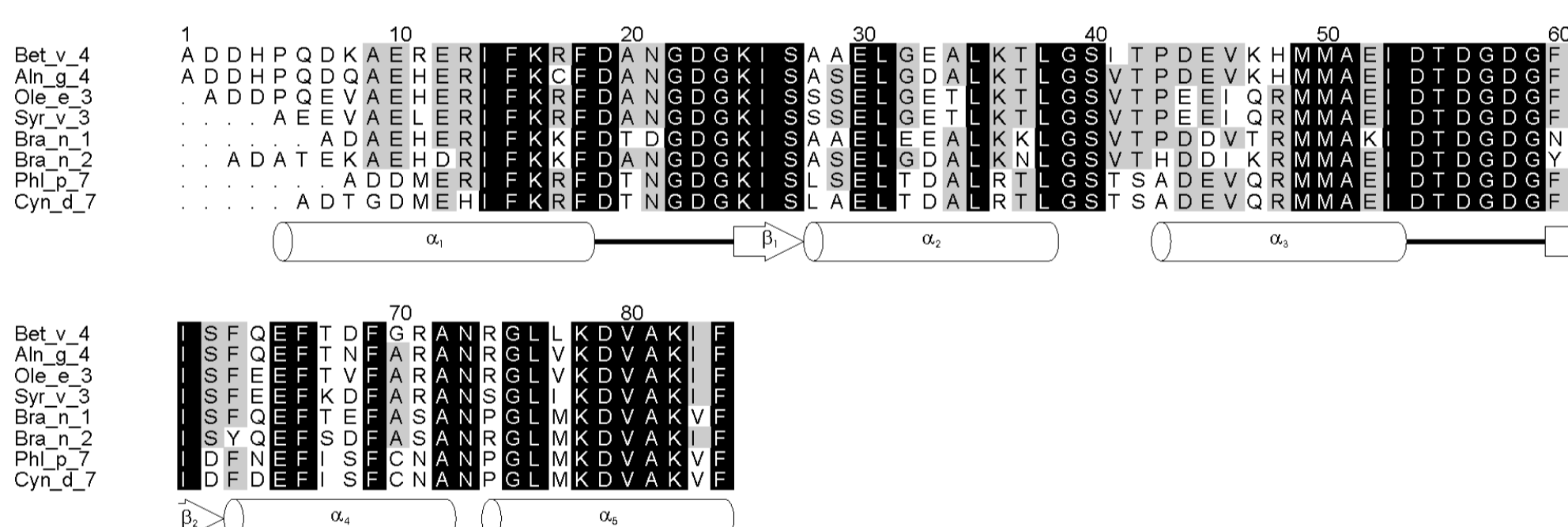


**Fig. 1:** Structure-based sequence alignment with Bet v 4 of Aln g 4 (89.3 % sequence identity to Bet v 4), Ole e 3 (79.5 %), Syr v 3 (77.5 %), Bra n 1 (74.4 %), Bra n 2 (73.2 %), Phl p 7 (68.8 %), and Cyn d 7 (68.4%). Bra r 1 and Bra r 2 are identical to Bra n 1 and Bra n 2, respectively. Note that with the exception of Bet v 4 and Ole e 3 these allergen designations have not been confirmed by the IUIS Allergen Nomenclature Sub-Committee yet and in the case of Bra n 1 and Bra r 2 even conflict with other allergens. The sequence positions above the sequences correspond to Bet v 4. Gaps in the alignment are indicated by dots. Residues conserved in at least 5 of the 8 allergens are highlighted by grey boxes, residues conserved in all 8 allergens by black boxes. The secondary structure elements of Bet v 4 are shown below the alignment and are identical to those of Phl p 7 except that the  $\text{NH}_2$ -terminal helix  $\alpha_1$  of Phl p 7 starts with Asp 2 corresponding to Ala 9 of Bet v 4. The two  $\text{Ca}^{2+}$  binding loops and the amphipathic COOH-terminal helix  $\alpha_5$  are particularly well conserved.

## Methods and Results

Analysis of a series of mostly heteronuclear multidimensional NMR experiments performed on both uniformly  $^{15}\text{N}$ - and uniformly  $^{13}\text{C}/^{15}\text{N}$ -labeled samples revealed a substantial but reversible transition of the tertiary structure upon  $\text{Ca}^{2+}$  binding responsible for the different IgE binding properties of apo and holo Bet v 4, and allowed identification of all of the well-dispersed 81 backbone amide resonances of holo Bet v 4 (Fig. 2). In total, we were able to determine 934 out of 1058 (88 %)  $^1\text{H}$ ,  $^{13}\text{C}$ , and  $^{15}\text{N}$  chemical shifts as well as 66  $^3\text{J}_{\text{NH}\alpha}$  scalar and 69  $^{\text{D}}\text{NH}$  dipolar coupling constants. Based on 1671 experimental restraints derived from these NMR experiments we determined the three-dimensional structure of holo Bet v 4 in solution (Fig. 3), which adopts a well-defined canonic calmodulin-like two EF-hand assembly (Fig. 4). The substantial transition of the tertiary structure upon  $\text{Ca}^{2+}$  binding (Fig. 2) resulting in the exposition of a hydrophobic groove (Fig. 5) strongly suggests a regulatory rather than a  $\text{Ca}^{2+}$  buffering function for Bet v 4. The dynamic and hydrodynamic properties analyzed by NMR relaxation, NMR translational diffusion and analytical ultracentrifugation measurements clearly show that both apo and holo Bet v 4 are predominantly monomeric under all conditions tested (Tab. 1), with only a small dimer fraction of about 15 % for holo Bet v 4, which did not reach equilibrium with the monomer in sedimentation-diffusion equilibrium ultracentrifugation measurements on the timescale of several hours (data not shown). In spite of their different oligomerization state the secondary and tertiary structure of Bet v 4 and Phl p 7 are remarkably similar (Fig. 6), thus providing a straightforward explanation for the observed immune cross-reactivity among the polcalcin family of allergens.

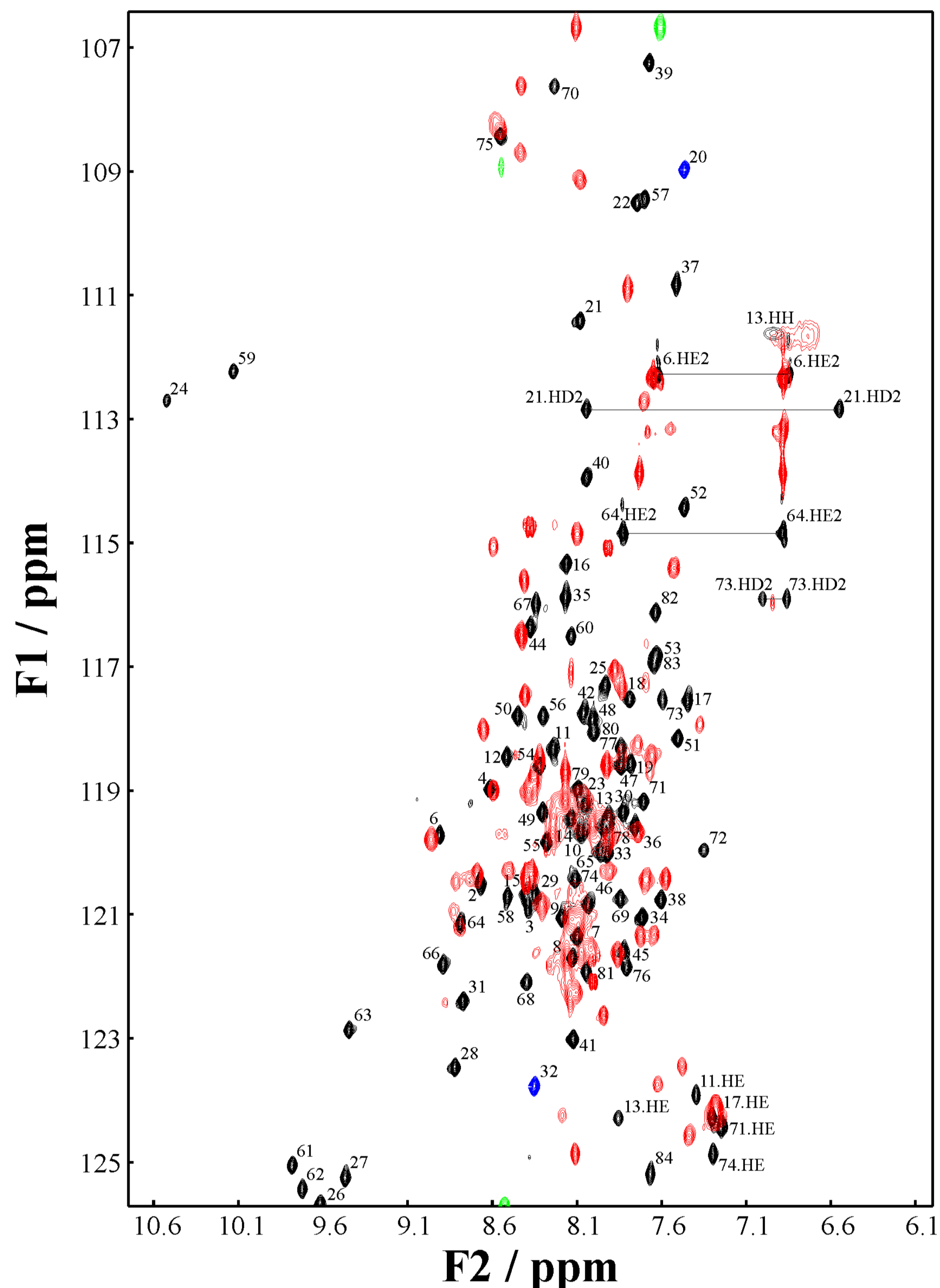


**Fig. 2:** Overlay of the  $^1\text{H}$ ,  $^{15}\text{N}$  HSQC spectra of 0.7 mM uniformly  $^{15}\text{N}$ -labeled apo Bet v 4 (positive signals in red, negative signals in green) and of 1.5 mM uniformly  $^{13}\text{C}/^{15}\text{N}$ -labeled holo Bet v 4 (positive signals in black, negative signals in blue) in 25 mM sodium acetate, pH = 6.0, 10 % (v/v)  $\text{D}_2\text{O}$ , recorded at T = 298 K on Bruker Avance400 and DMX750 NMR spectrometers, respectively. Upon depletion of  $\text{Ca}^{2+}$  ions the well-dispersed amide proton resonances of holo Bet v 4 labeled according to their residue numbers lose most of their chemical shift dispersion, especially those shifted to low field, which are all located in the  $\text{Ca}^{2+}$  binding loops. The chemical shift dispersion is restored completely upon addition of excess  $\text{CaCl}_2$  (data not shown), indicating a substantial but reversible transition of the tertiary structure, which explains the different IgE binding properties of apo and holo Bet v 4.

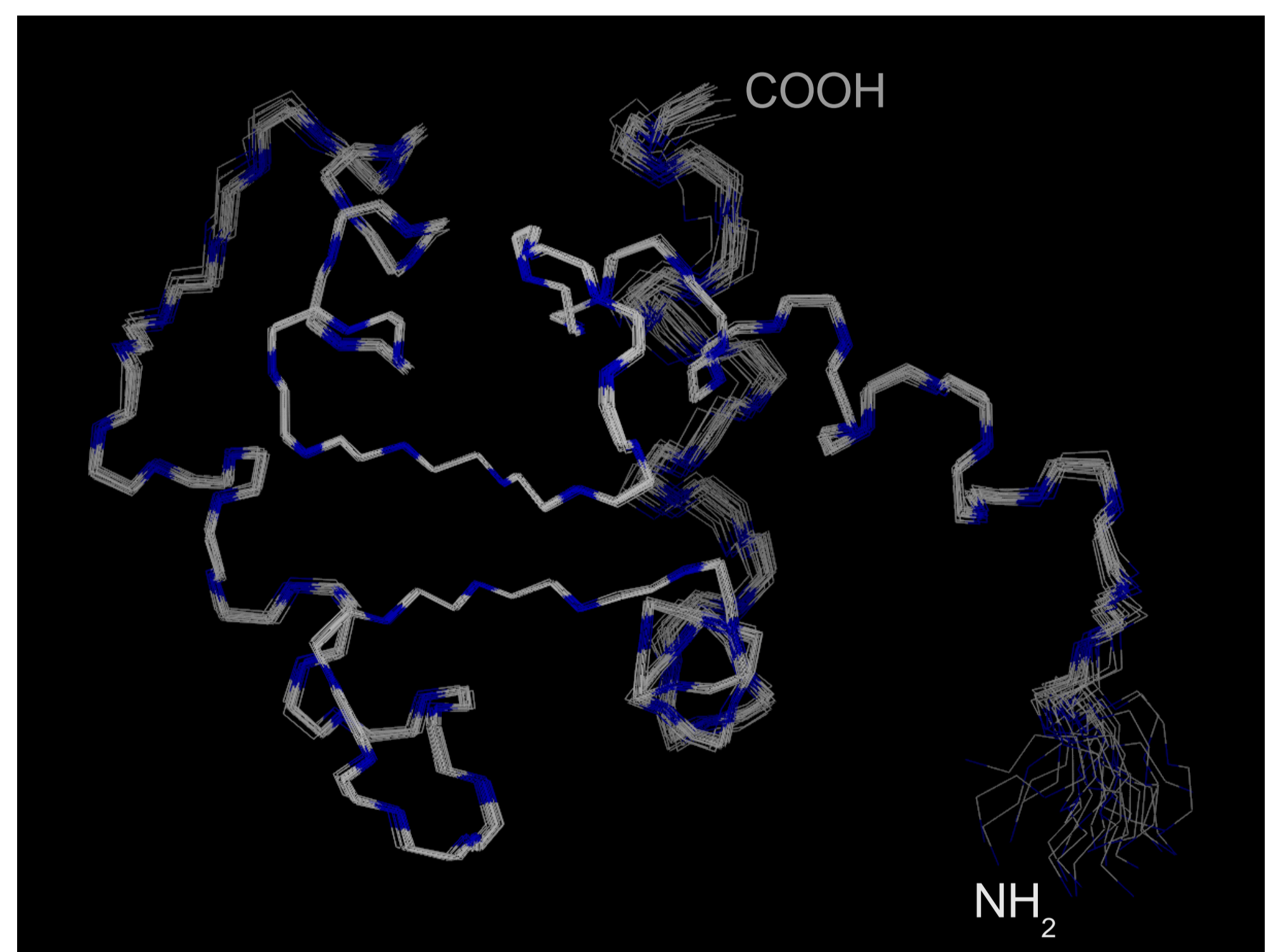


**Fig. 3:** Backbone overlay of the 25 accepted structures of holo Bet v 4. C and N atoms are color-coded gray and blue, respectively. Except for the  $\text{NH}_2$ -terminal residues from Ala 1 to His 4, which show markedly increased backbone flexibility as evidenced by our NMR relaxation data, holo Bet v 4 shows a well-defined structure in solution with average atomic root mean square deviations (RMSDs) from the average structure of 0.22 Å for the backbone and 0.57 Å for all heavy atoms for the residues from Pro 5 to Phe 84.

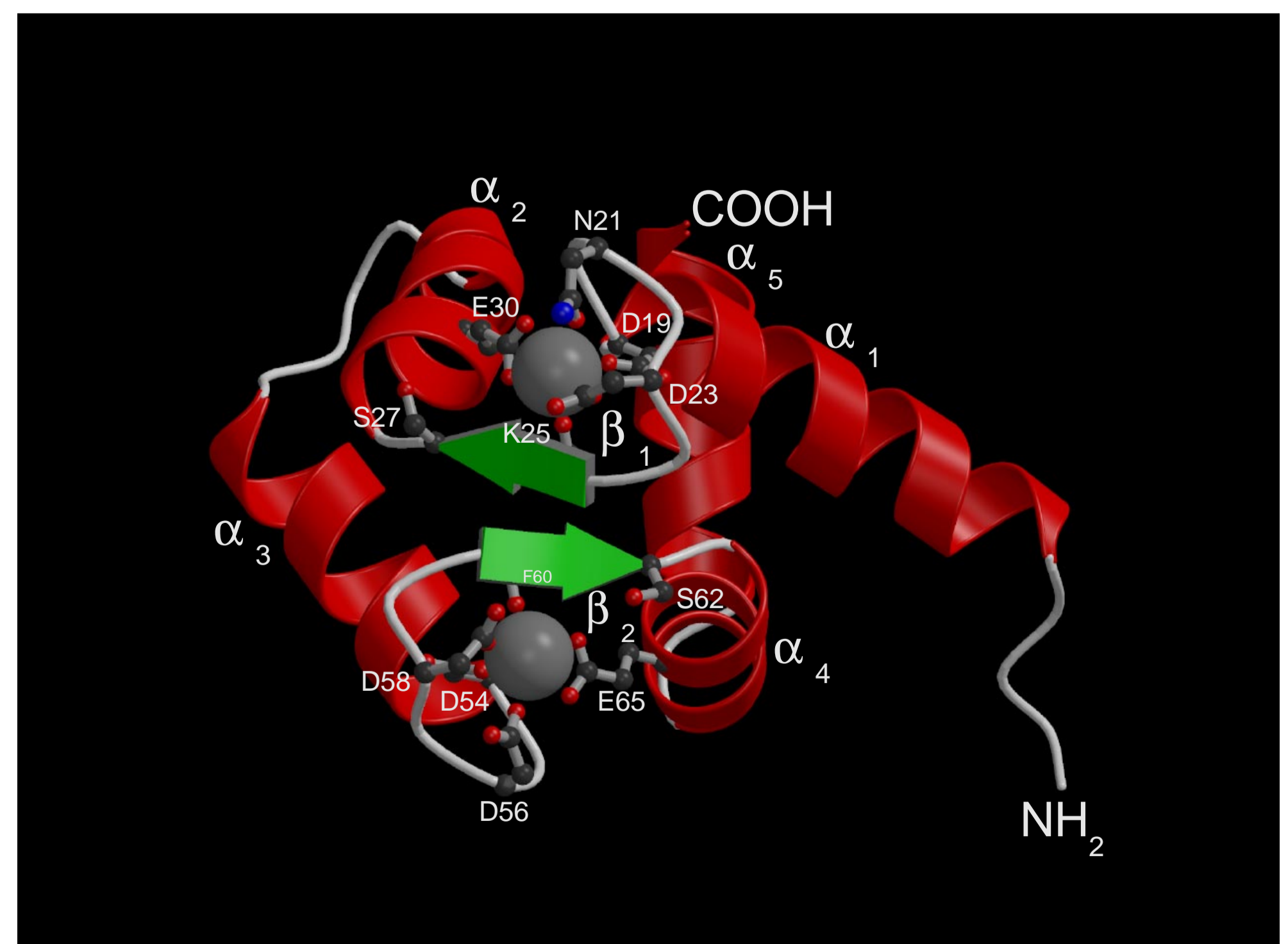


**Fig. 4:** Schematic representation of the secondary structure elements of holo Bet v 4. Same view as in Fig. 3. The helices  $\alpha_1$  and  $\alpha_2$  as well as  $\alpha_3$  and  $\alpha_4$  form two canonical EF-hands in the open conformation, with their interhelical angles of  $101.5^\circ \pm 0.9^\circ$  and  $96.9^\circ \pm 1.0^\circ$ , respectively, closely resembling those of holo calmodulin. The EF-hands are paired via a short two-stranded antiparallel  $\beta$ -sheet. The amphipathic COOH-terminal helix  $\alpha_5$  packs into the hydrophobic groove formed by the helices  $\alpha_1$  and  $\alpha_2$  (Fig. 5). The experimental data is consistent with a coordination of each of the two  $\text{Ca}^{2+}$  ions by six protein oxygen atoms of the residues shown in ball-and-stick-representation at the vertices of a pentagonal bipyramid as in calmodulin, which had to be modeled since due to lack of protons no experimental restraints for the coordination itself could be derived. A water molecule probably H-bonded to the slowly exchanging hydroxyl proton of Ser 27 or Ser 62 contributes the remaining coordination site each.

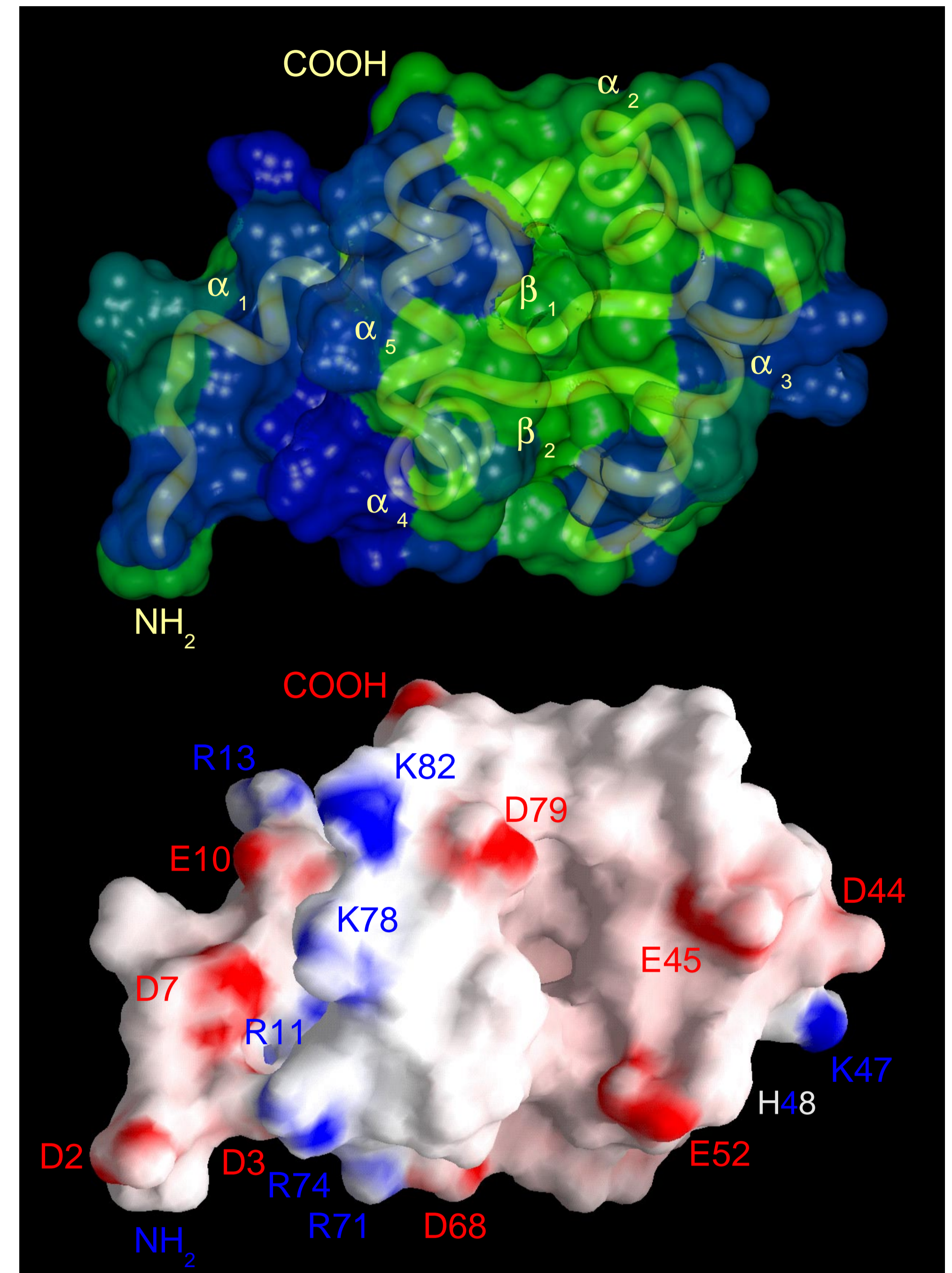


**Fig. 5:** Connolly surface of holo Bet v 4 colored according to hydrophobicity (top; hydrophobic residues green, hydrophilic residues blue) or electrostatic potential (bottom; negative potential red, positive potential blue). Opposite view as in Fig. 3 and 4. The electric charge of the side-chain of His 48 depends on pH, at pH = 6.0 it is predominantly protonated. The COOH-terminal helix  $\alpha_5$  does not cover the hydrophobic groove lined by negatively charged residues completely. Exposition of a similar hydrophobic ligand binding groove is the mechanistic purpose of the transition of the tertiary structure of calmodulin and troponin C upon  $\text{Ca}^{2+}$  binding, indicating that Bet v 4 serves a regulatory rather than a  $\text{Ca}^{2+}$  buffering function. Determination of the high-resolution three-dimensional structure of apo Bet v 4 and screening of potential ligands is currently under way in our laboratory. Formation of the domain-swapped dimer of holo Phl p 7 closes this hydrophobic groove, resulting in a hydrophobic cavity which is no longer solvent-accessible<sup>3</sup>.

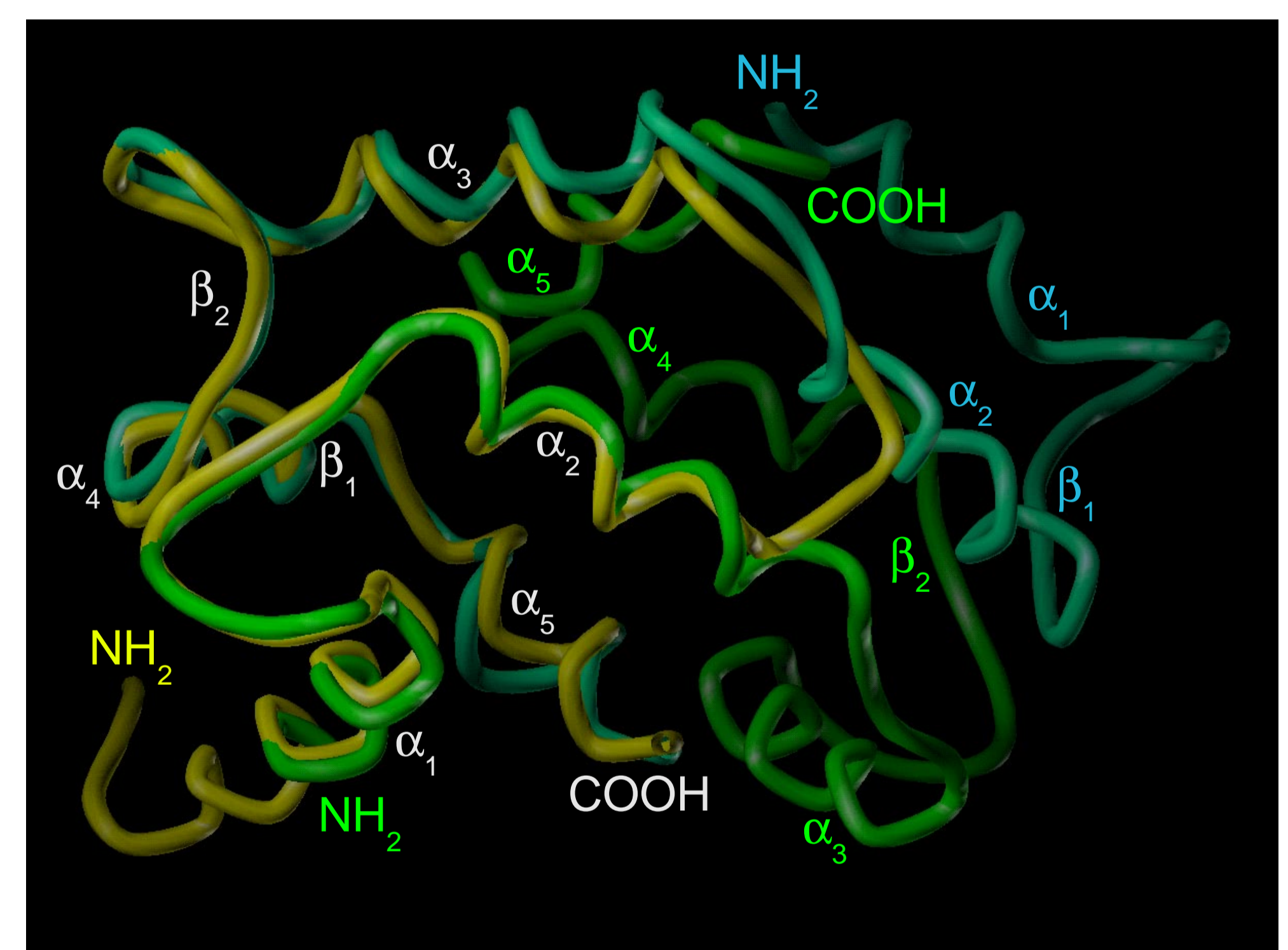


**Fig. 6:** Backbone overlay of the average solution structure of holo Bet v 4 (yellow) with the  $\text{NH}_2$ -terminal EF-hand of the first monomer (green) and the COOH-terminal EF-hand of the second monomer (green-blue) of the crystal structure of holo Phl p 7<sup>3</sup>. Apart from the domain-swapping dimerization the tertiary fold is almost identical with a backbone atomic RMSD of 1.30 Å excluding the four residues linking the helices  $\alpha_3$  and  $\alpha_4$  (Fig. 1). Surprisingly, this even holds for the COOH-terminal helix  $\alpha_5$  in spite of slight deformations caused by the tight intermolecular packing of holo Phl p 7<sup>3</sup>. Together with the high sequence identity (Fig. 1), the conserved backbone conformation leads to a very similar molecular surface as far as shape and charge distribution are concerned, rendering the existence of cross-reactive epitopes most likely.

		NMR <sup>a</sup>	Ultracentrifugation <sup>b</sup>	Calculation <sup>c</sup>
apo Bet v 4	Hydrodynamic radius	18.9 Å ± 0.4 Å	18.2 Å ± 0.1 Å	
	Hydrodynamic radius	17.8 Å ± 0.4 Å	17.9 Å ± 0.2 Å (= 85 %)	18.3 Å
holo Bet v 4	Overall rotational diffusion autocorrelation times	6.1 ns	22.2 Å ± 0.2 Å (= 15 %)	6.5 ns
		5.9 ns		6.2 ns
		5.4 ns		5.4 ns

**Tab. 1:** Hydrodynamic properties of apo and holo Bet v 4.

<sup>a</sup> NMR translational diffusion measurements relative to internal dioxane and overall rotational diffusion autocorrelation times from NMR longitudinal and transverse relaxation measurements assuming a prolate axially symmetric rotational diffusion tensor.

<sup>b</sup> Hydrodynamic radii from sedimentation velocity experiments assuming a hydration of 30 % (w/w). Values are average values over measurements at 3 different protein concentrations from 0.15 mM to 0.68 mM (apo Bet v 4) or 4 different protein concentrations from 0.12 mM to 0.60 mM (holo Bet v 4) in the form average value ± standard deviation. The resulting molecular mass estimates are 10.18 kDa ± 0.08 kDa, 10.52 kDa ± 0.22 kDa, and 20.3 kDa ± 1.0 kDa for apo Bet v 4, monomeric holo Bet v 4, and dimeric holo Bet v 4, respectively.

<sup>c</sup> Values calculated on the basis of a prolate ellipsoid of revolution with semi-axes of 19.5 Å and 13.6 Å, which has the same tensor of inertia as holo Bet v 4 in the prolate axially symmetric approximation, adding a hydration layer of 2.8 Å.

## References

- Engel, K., Richter, G., Obermeyer, P., Briza, A. J., Kungl, B., Simon, M., Auer, C., Ebner, H.-J., Rheinberger, M., Breitenbach and F. Ferreira, *J. Biol. Chem.* **272**, 28630-28637 (1997)
- A. Twardosz, B. Hayek, S. Seiberler, L. Vangelista, L. Elfman, H. Grönlund, D. Kraft and R. Valenta, *Biochem. Biophys. Res. Comm.* **239**, 197-204 (1997)
- P. Verdino, K. Westritschnig, R. Valenta and W. Keller, *EMBO J.* **21**, 5007-5016 (2002)